https://doi.org/10.22226/2410-3535-2022-4-428-432

Realizing ultrafine grain structure of Cu-Cr-Zr alloy via friction stir welding/processing

N. V. Lezhnin†,1, A. V. Makarov1, E. G. Volkova1, A. I. Valiullin1,
A. B. Kotelnikov2, A. A. Vopneruk2
†nlezhnin@bk.ru

1M. N. Mikheev Institute of Metal Physics UB RAS, Ekaterinburg, 620108, Russia
2MASHPROM, Ekaterinburg, 620143, Russia

40 mm thick coarse-grained (up to 10 – 20 mm) CuCrZr mold wall to 2 mm thick pure copper plate lap joint was performed using friction stir welding (FSW) operating a H13 die steel tool. The obtained defect-free joint indicates the potential of FSW to restore worn-out copper molds wall. FSW resulted in ultrafine microstructure (0.5 –1.0 μm) of stir zone strengthened by chromium and Cu_5Zr nanoparticles. Grain boundary and dispersion hardening increase the hardness of the stir zone up to 150 –190 HV1 compared to 110 –130 HV1 of the initial coarse-grained structure. Based on the results, friction stir welding and related friction stir processing technologies are proposed as a severe plastic deformation method to obtain an ultrafine-grained state of CuCrZr alloys.

Keywords: frictions stir welding/processing, CuCrZr alloy, intermetallic compound, structure, hardness.

1. Introduction

Chrome-zirconium bronze is a structural alloy widely used in the manufacture of equipment components in the metallurgical and power industries, as well as electronics [1 – 4]. The extremely low solubility of chromium and zirconium in copper at temperatures below 600°C allows one to achieve a high thermal and electrical conductivity of matrix hardened by nanoscale precipitations [4]. Cr ensures strengthening, while Zr increases the recrystallization temperature providing good heat resistance.

Severe plastic deformation is an effective way to improve the mechanical characteristics of material through grain refinement to submicron- and nanoscale. There are detailed studies of the structure and properties of copper processed by high pressure torsion [5 – 7] and chromium-zirconium bronze after equal-channel angular pressing [8], dynamic channel-angular pressing, and rolling [9 – 11]. Usually, obtaining a high-strength state of Cu-Cr-Zr alloy is a rather complex three-stage process including preliminary solution annealing and severe plastic deformation followed by aging.

Recently developed technologies of friction stir welding (FSW) and related friction stir processing (FSP) are essentially thermomechanical processes based on the concept of mechanical transfer of plasticized material around a rotating tool with a specially designed pin and shoulder inserted into a workpiece (Fig. 1). During the process, plastic deformation reaches hundreds of percent leading to grain refinement whereas heating contributes to dynamic recovery and recrystallization of a material.

Welding parameters significantly affect both the microstructure and the mechanical properties of a material.

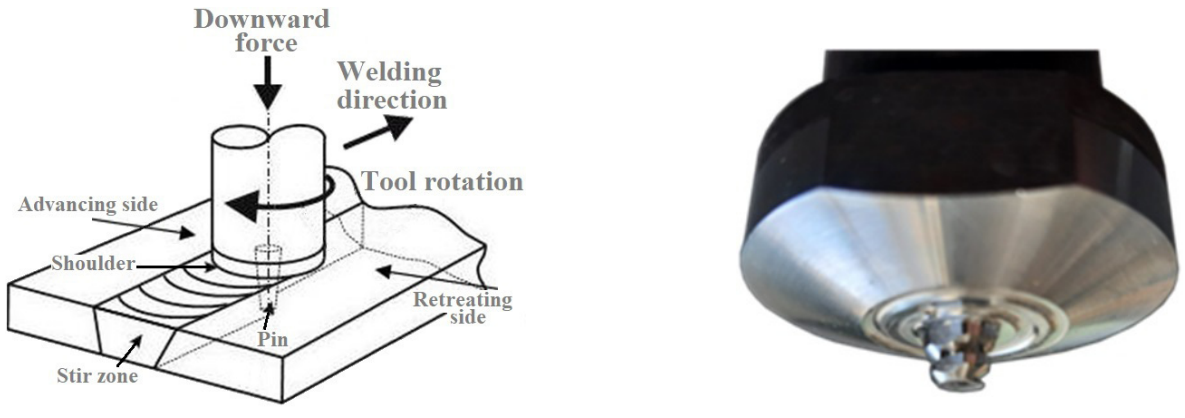

Fig. 1. Schematic drawing of friction stir welding/processing (a) and stir tool (b).

A number of works describe the features of structure evolution and precipitation behavior in Cu-Cr-Zr alloys during FSP/FSW [12–14]. It has been shown, that high heat input FSW/FSP causes grains growth, as well as coarsening and dissolution of hardening phases, which negatively affect the mechanical and physical properties of the material [13]. On the contrary, low-heat input FSW/FSP is a promising way to improve strength-conductivity combination owing to three aspects. Firstly, decreased heat input inhibits the growth of the recrystallized grains enhancing the strength via grain refining. Secondly, it could prevent coarsening or dissolution of dispersed phases, maintaining the precipitation strengthening effect and good conductivity. Lastly, the particles distributed in the matrix contribute to grain refinement, acting as nucleation sites and restraining grains growth. Certain modes of FSW are able to provide almost equal strength joining with high electrical and thermal conductivity [15,16].

Considering friction stir lap-welding as a restoration method of used-up mold walls of continuous-casting machines, it is of great interest to designate how FSW influences the structure and properties of coarse-grained Cu-Cr-Zr alloy, comprising large hardening phases. Therefore the work aims to study the structure, phase composition, and hardness of the stir zone of chromium-zirconium bronze mold wall after restoration by low heat input FSW.

2. Materials and experimental methods

40 mm thick chromium-zirconium bronze mold wall was used as a base material (BM). The chemical composition of bronze is given in Table 1. 2 mm thick pure copper (99.9 wt.% Cu) plate was used as a filler material.

FSW was carried out in IMP UB RAS using a portal friction stir welder. The die steel H13 (4Cr5MoVSi) stir tool with a conical threaded pin 5 mm in length, 8 mm in base diameter and 6 mm root diameter was employed (Fig. 1b). Single pass FSW parameters were selected as follows: load 20000 N, rotation speed 900 rpm, welding speed 0.5 mm/s, tilt angle 3°, air cooling. The temperature at the periphery of the stir zone was measured by a non-contact laser pyrometer. The measurement point was chosen at the edge of the tool shoulder near the workpiece surface. Microstructure in the transverse section of the stir zone was examined by optical microscopy (OM), scanning electron microscopy (SEM) and transmission electron microscopy (TEM). Specimens for OM observation were etched in 50% water solution of nitric acid. Hardness was measured on an automated hardness tester under a load of 1 kg.

3. Results and discussion

3.1. Macrostructure of stir zone

Figure 2 shows the cross-sectional macrographs of lap joint between mold wall and copper plate. The initial structure of the chromium-zirconium bronze mold wall (Fig. 2a) consists of coarse recrystallized grains reaching tens of millimeters in size. The weld stir zone (SZ) has a clear boundary and shape close to the tool pin geometry with a moderate shoulder-affected zone. It is believed to be due to the low heat input during FSW, high thermal conductivity and high deformation resistance of the material. No defects were found in the SZ and along the joint line between the plates. It indicates a continuous bonding of the base metal with the filler plate used to restore the thickness of the mold wall. Figure 2b demonstrates the complexity of metal flow around the tool with clearly distinguishable three centers of "onion rings" structure, typical for FSW.

3.2. Microstructure of stir zone

SEM images in Fig. 3a demonstrate massive particles distributed in the base material. The dark rounded particles 1–5 μm in size are pure chromium precipitates with bcc lattice [17,18], while light rod-shaped particles up to 1 μm in size are Cu_5Zr with a complex face-centered cubic lattice of the Be_5Au type [19,20]. On the other hand, high magnified TEM (Fig. 3b) reveals low dislocation density within the grains and almost complete absence of dispersed precipitations.

Table 1. Chemical composition of chrome-zirconium bronze.

Alloy	Ni	Cr	Cu	As	Zr	Pb	Zn	Bi	Sn	Impurities
CuCrZr	<0.03	0.4–1	98.82–99.57	<0.01	0.03–0.08	<0.003	<0.01	<0.002	<0.01	<0.1

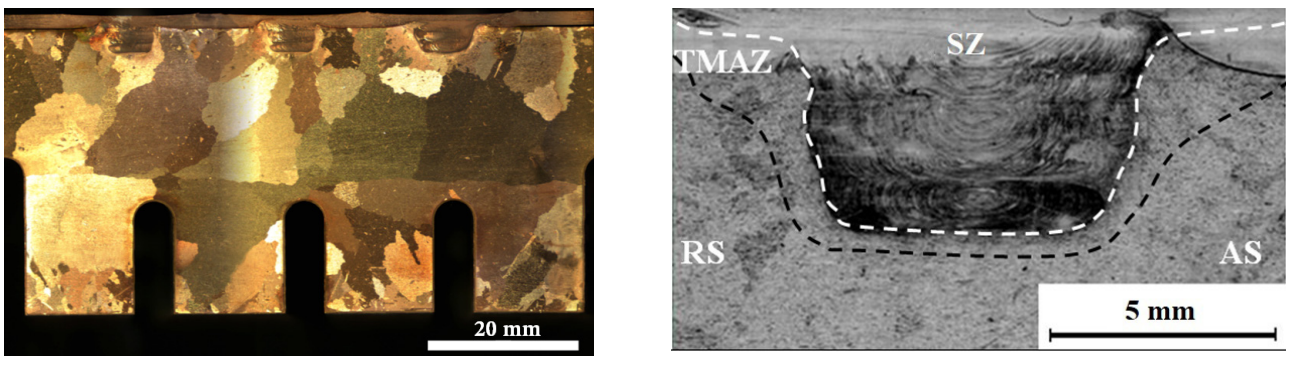

a b

Fig. 2. (Color online) Macrostructure of the base metal (a) and the cross-section of the stir zone between a filler plate (pure copper) and restored bronze base (b): AS — advancing side, RS — retreating side, SZ — stir zone, TMAZ — thermomechanically affected zone.

The stir zone (Fig. 4 a, c, d, e, f) has an ultrafine structure with crystallites and subgrains size in the range of 0.5 –1.0 μm, which is four orders of magnitude less compared to initial grains. The reflections in the microdiffraction patterns are points with a slight radial smearing (Fig. 4 b). The dark-field image in an 111γ reflection shows, that stir zone contains the arbitrary shape grains with gradually changing orientation (Fig. 4 c), the elastically distorted grains with irregular banded high-angle boundaries (Fig. 4 d), defect accumulation within the grain and the formation of a new high-angle boundary (Fig. 4 e), a recrystallization nucleus at the grain junction (Fig. 4 f). All these phenomena indicate the occurrence of dynamic recrystallization under conditions of heating of the stir zone by a rotating tool.

Nanoscale precipitates of chromium and Cu_5Zr from 3 to 20 nm in size were found in the stir zone (Fig. 4 g – i), which were not observed in the initial structure. Some chromium particles 3 – 5 nm in size retain coherent bonding with the matrix [16, 21], and could be visible in the matrix reflections in Fig. 4 c, h. Thus, the TEM data indicate the occurrence of

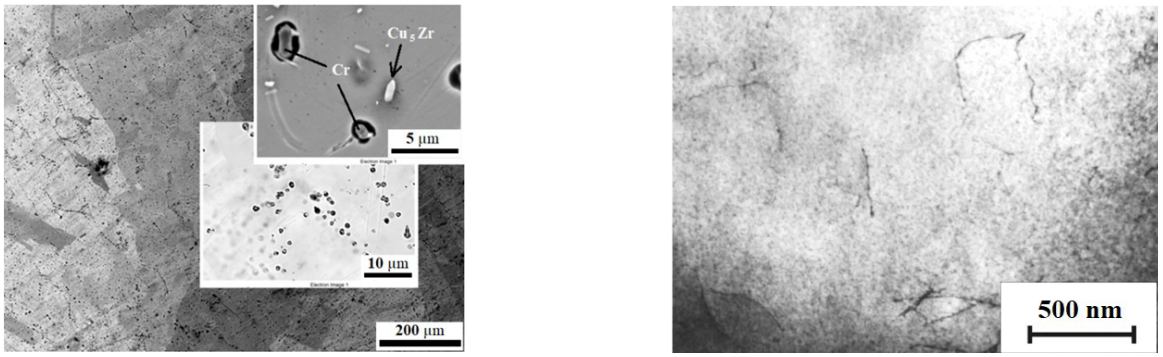

a b

Fig. 3. Initial microstructure of Cu-Cr-Zr plate SEM image (a) and TEM image (b).

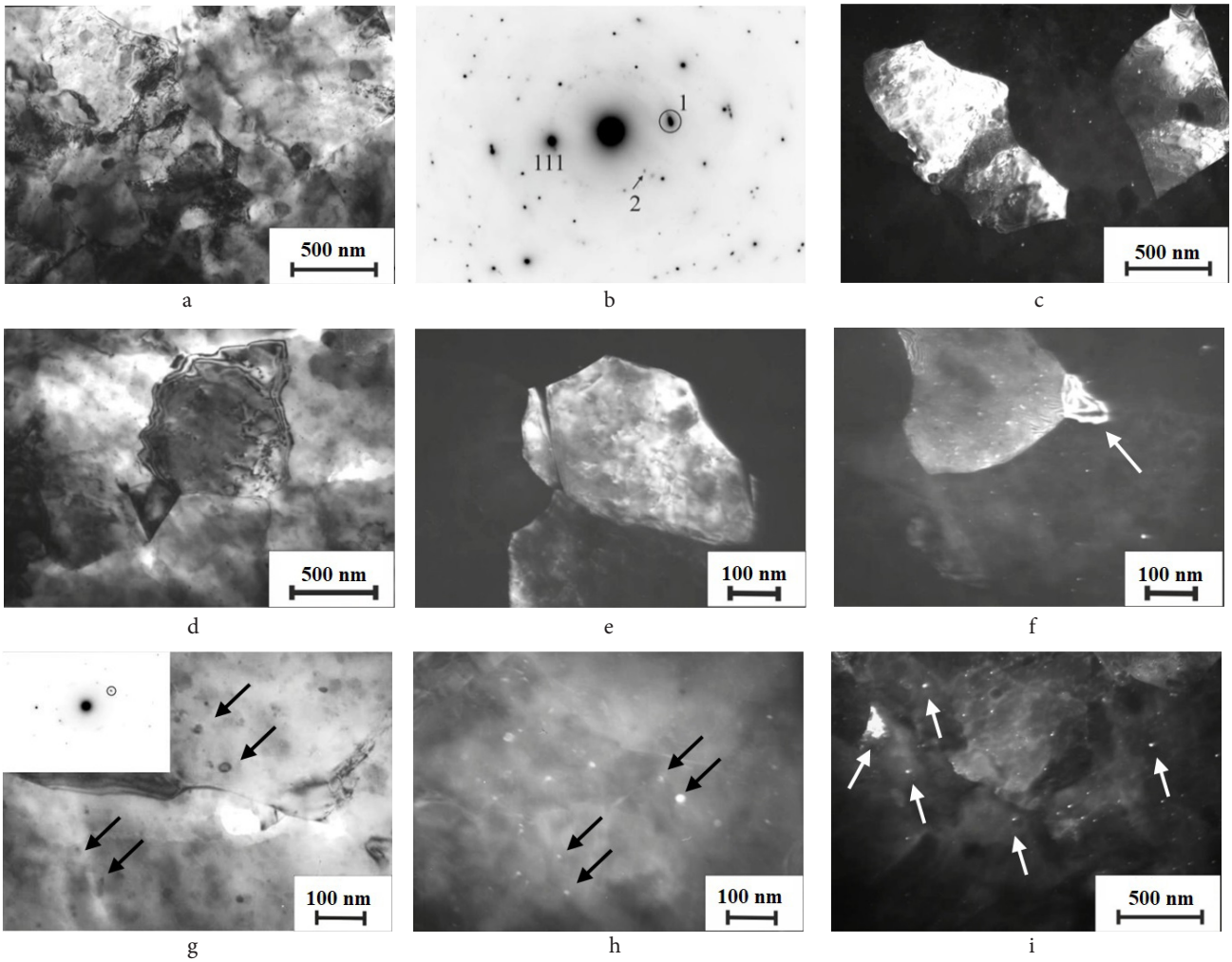

a b c d e f g h i

Fig. 4. The microstructure of Cu-Cr-Zr plate in the center of stir zone (TEM): bright-field image (a); microdiffraction pattern (b); dark-field image in a 111γ reflection (1) (c); streaky contrast at the grain boundary (d); formation of a high-angle boundary (e); formation of a recrystallization nucleus (f); chromium particles, bright-field image and microdiffraction pattern (g), the dark-field image in the 002γ reflection in Fig. 4 g (h), Cu_5Zr intermetallic particles, the dark-field image in a 220 Cu_5Zr reflection (2) in Fig. 4 b (i).

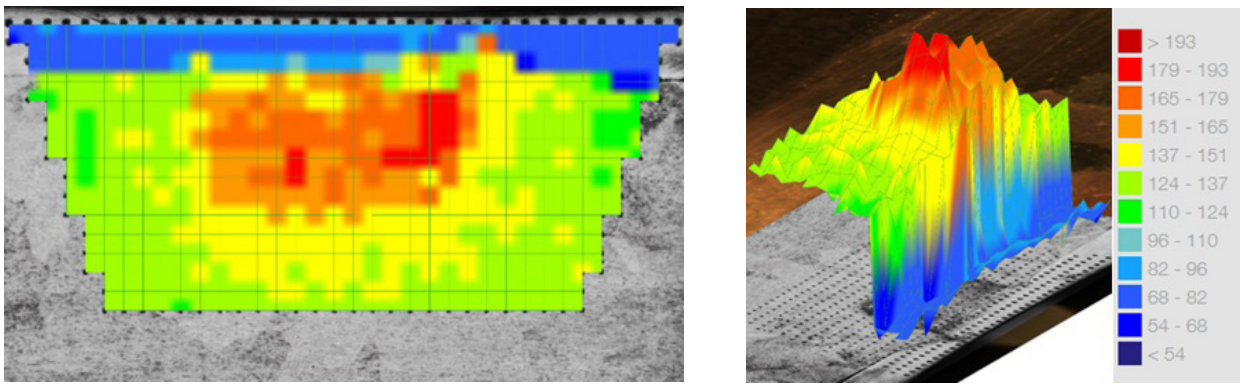

a b

Fig. 5. (Color online) Hardness distribution 2D-map (a) and 3D profile (b) of FSW zone HV1.

deformational dissolution of large phases during FSW with subsequent release of dispersed precipitates [22]. The density of precipitations is usually higher for such alloy composition [9]. The low density of nanoparticles could be associated with the incomplete transfer of chromium and zirconium from the initial hardening phases to a solid solution during the FSW. In Fig. 4 i, one can see a relatively coarse Cu_5Zr particle of irregular shape, probably subjected to partial dissolution, which confirms the incomplete dissolution of the initial particles.

The recorded temperature at the periphery of the FSW area was 280°C. According to the simulation results [13], the temperature in the stir zone is 100–150°C higher, thus reaching about 420°C. It is in agreement with the results of [9], where the precipitations 4–10 nm in size in ECAP bronze were observed only after annealing at temperatures of 400–450°C. The study of the microstructure testifies that FSW provides the Cr-Zr bronze structure refinement comparable to equal channel angular pressing and high-pressure torsion.

3.3. Hardness distribution

The hardness distribution map on the transverse cross-section for the FSW zone is presented in Fig. 5. The hardness of the coarse-grain base metal was between 110 and 130 HV1 (green). Strain hardening up to 137–151 HV1 occurred in the thermo-mechanically affected zone near the stir zone boundary (yellow). The hardness of the SZ was distributed in the range of 150–190 HV1 (red), which is 1.5–2 times higher, compared to coarse-grain base material. The hardness increase in the SZ zone could be explained by the grain-boundary hardening mechanism due to the ultrafine-grained state and enhanced dispersion hardening as a result of deformation dissolution chromium and Cu_5Zr phases followed by dispersive particles precipitation. The obtained hardness level is comparable with high strength Cu-Cr-Zr after a three-stage process, including dissolution, DCAP, and aging [9]. In this regard, FSW could be proposed as a less complex way to obtain an ultrafine-grained state of the Cu-Cr-Zr alloys.

4. Conclusions

The FSW was proposed as a thickness recovery method for mold wall of continuous-casting machines. The sound joint between the chromium-zirconium bronze base 40 mm thick and 2 mm pure copper plate was obtained by friction stir welding (FSW) operating an H13 steel tool.

The grain structure in the stir zone was refined by four orders of magnitude from 10–20 mm to 0.5–1.0 μm during single pass FSW. The stir zone contains nanoparticles of chromium and Cu_5Zr, which were not observed in the initial material.

The hardness of the stir zone (150–190 HV1) is 1.5–2.0 times higher compared to coarse-grain material (110–130 HV1) due to refinement of the grain structure and additional dispersion hardening coursed by partial dissolution of initial Cr and Cu_5Zr phases and subsequent precipitation of nanoparticles.

Thus, the FSW process can be successfully used either to join structural elements made of copper and copper alloys or as an effective way to achieve ultrafine-grained state of Cu-Cr-Zr alloys.

Acknowledgments. The research was carried out within the state assignment of Ministry of Science and Higher Education of the Russian Federation (theme "Structure" No. 122021000033-2).

References

1. V. R. Barabash, G. M. Kalinin, S. A. Fabritsiev, S. J. Zinkle. J. Nucl. Mater. 417 (1-3), 904 (2011). Crossref
2. C. Jinshui, Y. Bin, W. Junfeng, X. Xiangpeng, C. Huiming, W. Hang. Mater. Res. Express. 5 (2), 026515 (2018). Crossref
3. R. Li, E. Guo, Z. Chen, H. Kang, W. Wang, C. Zou, T. Wang. J Alloys Compd. 771, 1044 (2019). Crossref
4. N. Liang, J. Liu, S. Lin, Y. Wang, J. T. Wang, Y. Zhao, Y. Zhu. J Alloys Compd. 735, 1389 (2018). Crossref
5. D. K. Orlova, T. I. Chashchukhina, L. M. Voronova, M. V. Degtyarev. Phys. Metals Metallogr. 116, 951 (2015). Crossref
6. T. I. Chashchukhina, M. V. Degtyarev, L. M. Voronova. Phys. Metals Metallogr. 109, 201 (2010). Crossref
7. T. I. Chashchukhina, L. M. Voronova, M. V. Degtyarev, D. K. Pokryshkina. Phys. Metals Metallogr. 111, 304 (2011). Crossref
8. A. Vinogradov, V. Patlan, Y. Suzuki, K. Kitagawa, V. I. Kopylov. Acta Mater. 50, 1639 (2002). Crossref
9. V. I. Zel'dovich, S. V. Dobatkin, N. Yu. Frolova, I. V. Khomskaya,

A. E. Kheifets, E. V. Shorokhov. Phys. Metals Metallogr. 117 (1), 79 (2016). Crossref
10. V. I. Zel'dovich, I. V. Khomskaya, N. Yu. Frolova, A. E. Kheifets, E. V. Shorokhov, P. A. Nasonov. Phys. Metals Metallogr. 114 (5), 411 (2013). Crossref
11. V. I. Zel'dovich, N. Yu. Frolova, I. V. Khomskaya, A. E. Kheifets, E. V. Shorokhov, P. A. Nasonov. Phys. Metals Metallogr. 115 (5), 465 (2014). Crossref
12. R. Lai, D. He, G. He, J. Lin, Y. Sun. Metals. 7 (9), 381 (2017). Crossref
13. R. Lai, X. Li, D. He, J. Lin, J. Li, Q. Lei. J. Nucl. Mater. 510, 70 (2018). Crossref
14. R. B. Naik, K. V. Reddy, G. M. Reddy, R. A. Kumar. Fusion Eng. Design. 161, 111962 (2020). Crossref
15. Y. D. Wang, M. Liu, B. H. Yu, L. H. Wu, P. Xue, D. R. Ni, Z. Y. Ma. Mater. Process. Technol. 288, 116880 (2021). Crossref
16. Y. D. Wang, S. Z. Zhu, G. M. Xie, L. H. Wu, P. Xue, D. R. Ni, Z. Y. Ma. Sci. Technol. Weld. Joining. 26 (6), 448 (2021). Crossref
17. A. Chbihi, X. Sauvage, D. Blavette. Acta Mater. 60 (11), 4575 (2012). Crossref
18. A. Morozova, R. Mishnev, A. Belyakov, et al. Rev. Adv. Mater Sci. 54, 56 (2018). Crossref
19. Springer Materials Website
20. I. V. Khomskaya, V. I. Zel'dovich, N. Y. Frolova, D. N. Abdullina, A. E. Kheifets. Letters on Materials. 9 (4), 400 (2019). Crossref
21. L. J. Peng, H. F. Xie, G. J. Huang, et al. J Alloys Compd. 708, 1096 (2017). Crossref
22. G. R. Khalikova, G. R. Zakirova, A. I. Farkhutdinov, E. A. Korznikova, V. G. Trifonov. Letters on Materials. 12 (3), 255 (2022). Crossref